# A Frequency-Dependent Weakly Conditionally Stable Finite-Difference Time-Domain Method for Dispersive Materials

**Juan Chen[1, 2], Jianguo Wang [1, 2]**

[1]School of Electronic and Information Engineering
Xi'an Jiaotong University, Xi'an 710049, China
chenjuan0306@yahoo.com.cn

[2]Northwest Institute of Nuclear Technology
P. O. Box 69-15, Xi'an 710024, China

***Abstract* -** A frequency-dependent weakly conditionally stable finite-difference time-domain (WCS-FDTD) method for dispersive materials is presented. This method has higher computation efficiency than conventional FDTD method because the time step in this method is only determined by one space discretization. The accuracy of this method is demonstrated by computing the incident field at a planar air-water interface over a wide frequency band including the effects of the frequency-dependent permittivity of water.

***Index Terms* -** Dispersive materials, FDTD method, WCS-FDTD method.

## I. INTRODUCTION

The finite-difference time-domain (FDTD) method [1] has been proven to be an effective scheme that provides accurate predictions of field behaviors for varieties of electromagnetic interaction problems. However, as it is based on an explicit finite-difference algorithm, the Courant–Friedrich–Levy (CFL) condition [2] must be satisfied when this method is used. Therefore, a maximum time-step size is limited by the minimum cell size in a computational domain, which makes this method inefficient for the problems where fine scale structures are involved.

To overcome the CFL constraint on the time step size of the FDTD method, some unconditionally stable methods [3-6] and weakly conditionally stable (WCS) [7-21] schemes have been studied, among which, the WCS-FDTD method scheme, has been applied extensively [15-21]. In the WCS-FDTD method, the time step size is only determined by one space discretization, which is useful for problems with very fine structures in two directions. The accuracy and efficiency of this method have been well validated in [17] and [18].

In this paper, the WCS-FDTD method will be extended to frequency-dependent materials. The formulations of WCS-FDTD for a frequency-dependent complex permittivity are presented and an example calculation of the incident field at a planar air-water interface over a wide frequency band is showed. The extension of the WCS-FDTD method to frequency-dependent permeability is similar and straightforward.

## II. FORMULATIONS

For this paper, we will assume that our materials are linear and isotropic, and only the permittivity is frequency-dependent. Extension to nonlinear or anisotropic dispersive materials should be possible. The displacement vector $D$ is related to the electric field $E$ in the time domain by the following equation:

$$\begin{aligned} D(t) &= \varepsilon_\infty \varepsilon_0 E(t) \\ &+\varepsilon_0 \int_0^t E(t-\tau)\chi(\tau)\,d\tau. \end{aligned} \tag{1}$$

$\varepsilon_0$ is permittivity of free space, $\chi(\tau)$ is the electric susceptibility, and $\varepsilon_\infty$ is the infinite frequency relative permittivity.

Using Yee's notation, we let $t = n\Delta t$ in (1), and each vector component of $D$ and $E$ can be written as:

$$D(t) \approx D(n\Delta t) = D^n = \varepsilon_\infty \varepsilon_0 E^n + \varepsilon_0 \int_0^{n\Delta t} E(n\Delta t - \tau)\chi(\tau) d\tau. \quad (2)$$

All field components are assumed to be constant over each time interval $\Delta t/2$. Therefore, we have, assuming $D(t)$ and $E(t)$ are zero for $t < 0$:

$$D^n = \varepsilon_\infty \varepsilon_0 E^n + \varepsilon_0 \sum_{m=0}^{2n-1} E^{n-m/2} \int_{m\Delta t/2}^{(m+1)\Delta t/2} \chi(\tau) d\tau. \quad (3)$$

$$D^{n+1/2} = \varepsilon_\infty \varepsilon_0 E^{n+1/2} + \varepsilon_0 \sum_{m=0}^{2n} E^{n+1/2-m/2} \int_{m\Delta t/2}^{(m+1)\Delta t/2} \chi(\tau) d\tau. \quad (4)$$

$$D^{n+1} = \varepsilon_\infty \varepsilon_0 E^{n+1} + \varepsilon_0 \sum_{m=0}^{2n+1} E^{n+1-m/2} \int_{m\Delta t/2}^{(m+1)\Delta t/2} \chi(\tau) d\tau. \quad (5)$$

When (3) is substituted in (4), and (4) is substituted in (5), we find:

$$D^{n+1/2} - D^n = \varepsilon_\infty \varepsilon_0 \left[ E^{n+1/2} - E^n \right] + \varepsilon_0 E^{n+1/2} \int_0^{\Delta t/2} \chi(\tau) d\tau + \varepsilon_0 \sum_{m=0}^{2n-1} E^{n-m/2} \left\{ \begin{array}{l} \int_{(m+1)\Delta t/2}^{(m+2)\Delta t/2} \chi(\tau) d\tau \\ -\int_{m\Delta t/2}^{(m+1)\Delta t/2} \chi(\tau) d\tau \end{array} \right\}. \quad (6)$$

$$D^{n+1} - D^{n+1/2} = \varepsilon_\infty \varepsilon_0 \left[ E^{n+1} - E^{n+1/2} \right] + \varepsilon_0 E^{n+1} \int_0^{\Delta t/2} \chi(\tau) d\tau + \varepsilon_0 \sum_{m=0}^{2n} E^{n+1/2-m/2} \left\{ \begin{array}{l} \int_{(m+1)\Delta t/2}^{(m+2)\Delta t/2} \chi(\tau) d\tau \\ -\int_{m\Delta t/2}^{(m+1)\Delta t/2} \chi(\tau) d\tau \end{array} \right\}. \quad (7)$$

For simplicity, we let:

$$\chi_m = \int_{m\Delta t/2}^{(m+1)\Delta t/2} \chi(\tau) d\tau. \quad (8)$$

$$\Delta\chi_m = \chi_m - \chi_{m+1}. \quad (9)$$

Then, we have:

$$E^{n+1/2} = \varepsilon_\infty E^n / (\varepsilon_\infty + \chi_0) + \sum_{m=0}^{2n-1} E^{n-m/2} \Delta\chi_m / (\varepsilon_\infty + \chi_0) + \left( D^{n+1/2} - D^n \right) / (\varepsilon_\infty + \chi_0) \varepsilon_0. \quad (10)$$

$$E^{n+1} = \varepsilon_\infty E^{n+1/2} / (\varepsilon_\infty + \chi_0) + \sum_{m=0}^{2n} E^{n+1/2-m/2} \Delta\chi_m / (\varepsilon_\infty + \chi_0) + \left( D^{n+1} - D^{n+1/2} \right) / (\varepsilon_\infty + \chi_0) \varepsilon_0. \quad (11)$$

The three scalar equations that relate the components of electric field $E$ can be readily obtained from the WCS-FDTD method:

$$\begin{aligned} E_x^{n+\frac{1}{2}}\left(i+\frac{1}{2}, j, k\right) = {} & \frac{\varepsilon_\infty}{(\varepsilon_\infty + \chi_0)} E_x^n\left(i+\frac{1}{2}, j, k\right) + \frac{1}{(\varepsilon_\infty + \chi_0)} \sum_{m=0}^{2n-1} E_x^{n-\frac{m}{2}}\left(i+\frac{1}{2}, j, k\right) \Delta\chi_m \\ & + \frac{\Delta t}{(\varepsilon_\infty + \chi_0)\varepsilon_0} \frac{1}{\Delta y} \left[ \begin{array}{l} H_z^n\left(i+\frac{1}{2}, j+\frac{1}{2}, k\right) \\ -H_z^n\left(i+\frac{1}{2}, j-\frac{1}{2}, k\right) \end{array} \right] \\ & - \frac{\Delta t}{(\varepsilon_\infty + \chi_0)\varepsilon_0} \frac{1}{2\Delta z} \left[ \begin{array}{l} H_y^{n+\frac{1}{2}}\left(i+\frac{1}{2}, j, k+\frac{1}{2}\right) \\ -H_y^{n+\frac{1}{2}}\left(i+\frac{1}{2}, j, k-\frac{1}{2}\right) \\ +H_y^n\left(i+\frac{1}{2}, j, k+\frac{1}{2}\right) \\ -H_y^n\left(i+\frac{1}{2}, j, k-\frac{1}{2}\right) \end{array} \right]. \end{aligned} \quad (12)$$

$$
\begin{aligned}
&E_y^{n+\frac{1}{2}}\left(i, j+\frac{1}{2}, k\right) \\
&= \frac{\varepsilon_\infty}{(\varepsilon_\infty + \chi_0)} E_y^n\left(i, j+\frac{1}{2}, k\right) \\
&+ \frac{1}{(\varepsilon_\infty + \chi_0)} \sum_{m=0}^{2n-1} E_y^{n-\frac{m}{2}}\left(i, j+\frac{1}{2}, k\right)\Delta\chi_m \\
&- \frac{\Delta t}{(\varepsilon_\infty + \chi_0)\varepsilon_0} \frac{1}{2\Delta x}
\begin{bmatrix}
H_z^{n+\frac{1}{2}}\left(i+\frac{1}{2}, j+\frac{1}{2}, k\right) \\
-H_z^{n+\frac{1}{2}}\left(i-\frac{1}{2}, j+\frac{1}{2}, k\right) \\
+H_z^n\left(i+\frac{1}{2}, j+\frac{1}{2}, k\right) \\
-H_z^n\left(i-\frac{1}{2}, j+\frac{1}{2}, k\right)
\end{bmatrix}.
\end{aligned} \tag{13}
$$

$$
\begin{aligned}
&E_z^{n+\frac{1}{2}}\left(i, j, k+\frac{1}{2}\right) \\
&= \frac{\varepsilon_\infty}{(\varepsilon_\infty + \chi_0)} E_z^n\left(i, j, k+\frac{1}{2}\right) + \\
&\frac{1}{(\varepsilon_\infty + \chi_0)} \sum_{m=0}^{2n-1} E_z^{n-\frac{m}{2}}\left(i, j, k+\frac{1}{2}\right)\Delta\chi_m.
\end{aligned} \tag{14}
$$

$$
\begin{aligned}
&E_x^{n+1}\left(i+\frac{1}{2}, j, k\right) \\
&= \frac{\varepsilon_\infty}{(\varepsilon_\infty + \chi_0)} E_x^{n+\frac{1}{2}}\left(i+\frac{1}{2}, j, k\right) \\
&+ \frac{1}{(\varepsilon_\infty + \chi_0)} \sum_{m=0}^{2n} E_z^{n+\frac{1}{2}-\frac{m}{2}}\left(i+\frac{1}{2}, j, k\right)\Delta\chi_m.
\end{aligned} \tag{15}
$$

$$
\begin{aligned}
&E_y^{n+1}\left(i, j+\frac{1}{2}, k\right) \\
&= \frac{\varepsilon_\infty}{(\varepsilon_\infty + \chi_0)} E_y^{n+\frac{1}{2}}\left(i, j+\frac{1}{2}, k\right) \\
&+ \frac{1}{(\varepsilon_\infty + \chi_0)} \sum_{m=0}^{2n} E_y^{n+\frac{1}{2}-\frac{m}{2}}\left(i, j+\frac{1}{2}, k\right)\Delta\chi_m \\
&+ \frac{\Delta t}{(\varepsilon_\infty + \chi_0)\varepsilon_0} \frac{1}{2\Delta z}
\begin{bmatrix}
H_x^{n+1}\left(i, j+\frac{1}{2}, k+\frac{1}{2}\right) \\
-H_x^{n+1}\left(i, j+\frac{1}{2}, k-\frac{1}{2}\right) \\
+H_x^{n+\frac{1}{2}}\left(i, j+\frac{1}{2}, k+\frac{1}{2}\right) \\
-H_x^{n+\frac{1}{2}}\left(i, j+\frac{1}{2}, k-\frac{1}{2}\right)
\end{bmatrix}.
\end{aligned} \tag{16}
$$

$$
\begin{aligned}
&E_z^{n+1}\left(i, j, k+\frac{1}{2}\right) \\
&= \frac{\varepsilon_\infty}{(\varepsilon_\infty + \chi_0)} E_z^{n+\frac{1}{2}}\left(i, j, k+\frac{1}{2}\right) \\
&+ \frac{1}{(\varepsilon_\infty + \chi_0)} \sum_{m=0}^{2n} E_z^{n+\frac{1}{2}-\frac{m}{2}}\left(i, j, k+\frac{1}{2}\right)\Delta\chi_m \\
&- \frac{\Delta t}{(\varepsilon_\infty + \chi_0)\varepsilon_0} \frac{1}{\Delta y}
\begin{bmatrix}
H_x^{n+\frac{1}{2}}\left(i, j+\frac{1}{2}, k+\frac{1}{2}\right) \\
-H_x^{n+\frac{1}{2}}\left(i, j-\frac{1}{2}, k+\frac{1}{2}\right)
\end{bmatrix} \\
&+ \frac{\Delta t}{(\varepsilon_\infty + \chi_0)\varepsilon_0} \frac{1}{2\Delta x}
\begin{bmatrix}
H_y^{n+1}\left(i+\frac{1}{2}, j, k+\frac{1}{2}\right) \\
-H_y^{n+1}\left(i-\frac{1}{2}, j, k+\frac{1}{2}\right) \\
+H_y^{n+\frac{1}{2}}\left(i+\frac{1}{2}, j, k+\frac{1}{2}\right) \\
-H_y^{n+1/2}\left(i-\frac{1}{2}, j, k+\frac{1}{2}\right)
\end{bmatrix}.
\end{aligned} \tag{17}
$$

It can be seen from these equations that equations (12), (13), (16), and (17) can't be used for direct numerical calculation, because they all include the unknown components defined at the same time, thus, modified equations are derived from the original equations.

Updating of $E_x^{n+1/2}$ component, as shown in equation (12), needs the unknown $H_y^{n+1/2}$ component at the same time. In the nonmagnetic media, the updating for $H$ component is unchanged. The equation of the $H_y^{n+1/2}$ component in the WCS-FDTD method is as follows:

$$
\begin{aligned}
&H_y^{n+\frac{1}{2}}\left(i+\frac{1}{2}, j, k+\frac{1}{2}\right) \\
&= H_y^n\left(i+\frac{1}{2}, j, k+\frac{1}{2}\right) \\
&- \frac{\Delta t}{2\mu\Delta z}
\begin{bmatrix}
E_x^{n+\frac{1}{2}}\left(i+\frac{1}{2}, j, k+1\right) \\
-E_x^{n+1/2}\left(i+\frac{1}{2}, j, k\right) \\
+E_x^n\left(i+\frac{1}{2}, j, k+1\right) \\
-E_x^n\left(i+\frac{1}{2}, j, k\right)
\end{bmatrix}.
\end{aligned} \tag{18}
$$

Thus the $E_x^{n+1/2}$ component has to be updated implicitly. Substituting equation (18) into equation (12), the equation for $E_x^{n+1/2}$ field is given as,

$$\begin{aligned}
&(1+2\eta s)E_x^{n+1/2}\left(i+\frac{1}{2},j,k\right) \\
&-\eta s E_x^{n+1/2}\left(i+\frac{1}{2},j,k+1\right) \\
&-\eta s E_x^{n+1/2}\left(i+\frac{1}{2},j,k-1\right) \\
&=\eta\varepsilon_\infty E_x^{n}\left(i+\frac{1}{2},j,k\right) \\
&+\eta\sum_{m=0}^{2n-1}E_x^{n-\frac{m}{2}}\left(i+\frac{1}{2},j,k\right)\Delta\chi_m \\
&-2\eta s E_x^{n}\left(i+\frac{1}{2},j,k\right) \\
&+\eta s E_x^{n}\left(i+\frac{1}{2},j,k+1\right) \\
&+\eta s E_x^{n}\left(i+\frac{1}{2},j,k-1\right) \\
&+\eta\frac{\Delta t}{\varepsilon\Delta y}\begin{bmatrix}H_z^n\left(i+\frac{1}{2},j+\frac{1}{2},k\right) \\ -H_z^n\left(i+\frac{1}{2},j-\frac{1}{2},k\right)\end{bmatrix} \\
&-\eta\frac{\Delta t}{\varepsilon\Delta z}\begin{bmatrix}H_y^n\left(i+\frac{1}{2},j,k+\frac{1}{2}\right) \\ -H_y^n\left(i+\frac{1}{2},j,k-\frac{1}{2}\right)\end{bmatrix}
\end{aligned} \tag{19}$$

where $\eta = 1/(\varepsilon_\infty + \chi_0)$. $s = \Delta t^2/4\varepsilon\mu\Delta z^2$ .

The stability condition of the frequency dependent WCS-FDTD method is same as that of standard WCS-FDTD method,

$$\Delta t \le \frac{\Delta y}{c}. \tag{20}$$

Because in the frequency-dependent WCS-FDTD method equation, only a summation is added, it does not affect the stability condition.

The stability condition of the frequency dependent WCS-FDTD method will be validated by numerical example in the next section.

## III. NUMERICAL VALIDATION

In order to demonstrate the validity and accuracy of the above formulation, a small current source incident at a planar air-water interface is presented here. The geometric configuration of the numerical simulation is shown in Fig.1. The dimension of the perfect-electric-conductor box is 15cm ×3cm ×3cm. The water with the height 1.5cm is filled in the box. A small current source applied along $y$ direction is placed at the upper part of the box. The time dependence of the excitation function is:

$$g(t) = \exp[-4\pi(t-t_0)^2/t_1^2] \tag{21}$$

where $t_0$ and $t_1$ are constants, and both equal to $0.6\times10^{-9}$. The observation point B is set at the water, and 2.4 cm far from the source point A.

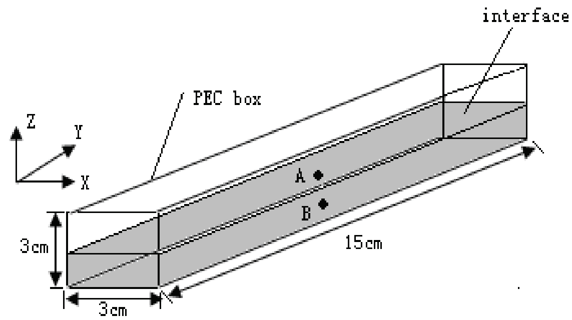


Fig. 1. Geometric configuration of the numerical simulation.

Applying the FDTD method to compute the time domain electric field component $E_y$ at observation point B, the cell size is chosen as $\Delta y = 5\Delta x = 5\Delta z =$ 0.5cm, so that the computational domain is 30 ×30 ×30 cells. To satisfy the stability condition of the FDTD algorithm, the time-step size for conventional FDTD [22] is $\Delta t \le 2.33$ps. For the WCS-FDTD scheme, the maximum time increment is only related to the space increments $\Delta y$ , that is, $\Delta t \le 16.66$ ps.

For water, the complex permittivity $\varepsilon^*(\omega)$ can be described as

$$\varepsilon^*(\omega) = \varepsilon_0\left[\varepsilon_\infty + (\varepsilon_s - \varepsilon_\infty)/(1+j\omega\tau_0)\right] \tag{22}$$

where $\varepsilon_s$ is the "static" permittivity, and $\tau_0$ is the "relaxation time" constant. The water parameters used here are $\varepsilon_s$ =81, $\varepsilon_\infty$ =1.8, and $\tau_0 = 9.4\times10^{-12}$ .

The summation (convolution) term of equations (10) and (11) can be updated recursively by utilizing equation (20) in [21], because the susceptibility function is an exponential. So, it does not require storing a large number of past time values $E^n$, and the computational time is saved. Only one additional number needs to be stored for each electric field component at each spatial index.

First, we validate the numerical stability of equation (19). Figure 2 shows the electric field component $E_y$ at observation point B calculated by using the WCS-FDTD methods with the time-step size $\Delta t$ =16.66 ps for a long time history. No instability problem is observed even for 5,000 time steps, which validates the weakly conditional stability of the WCS-FDTD method numerically.

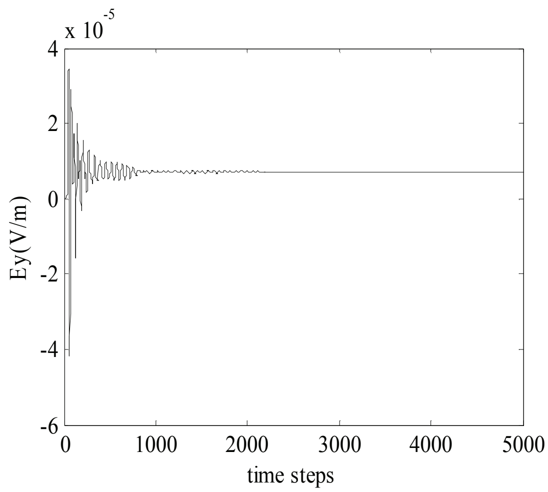


Fig. 2. The electric field component $E_y$ at observation point B calculated by using the WCS -FDTD method with the time-step size $\Delta t$ =16.66ps for a long time story.

To demonstrate the high computational efficiency of WCS-FDTD method, we perform the numerical simulations for an 8 ns time history by using the conventional FDTD, and WCS-FDTD methods, and compare the CPU times taken by using these two methods. In the conventional FDTD method, the time-step size is 2.33 ps, while in the WCS-FDTD method, the time step size is 16.66ps.

Figures 3 and 4 show the electric field component $E_y$ in the time domain and frequency domain at observation point B calculated by using the conventional FDTD, and WCS-FDTD methods. It can be seen from these figures that the result calculated by the WCS-FDTD method agrees with the result calculated by the conventional FDTD method. The WCS-FDTD method has almost the same accuracy as that of the conventional FDTD method, while, the simulation takes 206.94 s for the conventional FDTD method and 56.79s for the WCS-FDTD method. The time cost for the WCS-FDTD simulation is almost 1/4 times as that for the conventional FDTD simulation. So, we can conclude that the WCS-FDTD has higher efficiency than the conventional FDTD method, due to the use of larger time step size.

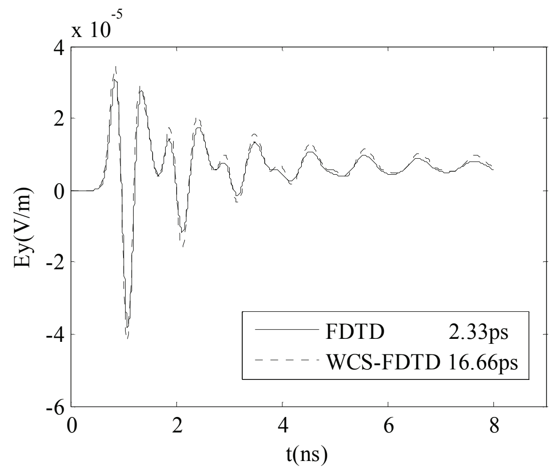


Fig. 3. The electric field component $E_y$ in the time domain at observation point B calculated by using the conventional FDTD ( $\Delta t$ =2.33ps), and WCS-FDTD methods ( $\Delta t$ =16.66ps).

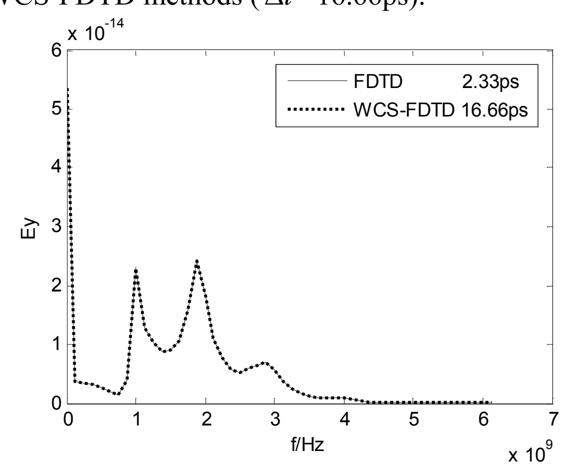


Fig. 4. The electric field component $E_y$ in the frequency domain at observation point B calculated by using the conventional FDTD $(\Delta t = 2.33\text{ps})$, and WCS-FDTD methods ( $\Delta t$ =16.66ps).

## IV. CONCLUSION

A frequency-dependent WCS-FDTD method for dispersive materials is presented. It is found that the technique is weakly conditionally stable and supports time steps greater than the CFL limit. Numerical example demonstrates that the computation efficiency of the WCS-FDTD method is higher than the conventional FDTD method, and the accuracy of the WCS-FDTD is almost the same as that of the conventional FDTD method.

## ACKNOWLEDGMENT

This work was supported by the Research Fund for the Doctoral Program of Higher Education of China (20090201120030), and also supported by the Basic Fund of Xi'an Jiaotong University.

## REFERENCES

[1] K. S. Yee, "Numerical solution of initial boundary value problems involving Maxwell's equations in isotropic media," *IEEE Trans. Antennas Propagat.*, vol. 14, pp. 302–307, May 1966.

[2] A. Taflove, *Computational Electrodynamics,* Artech House, 1995.

[3] F. Zheng, Z. Chen, and J. Zhang, "A finite-difference time-domain method without the Courant stability conditions," *IEEE Microwave Guided. Wave Lett.*, vol. 9, pp. 441–443, Nov. 1999.

[4] T. Namiki, "3-D ADI-FDTD scheme-unconditionally stable time-domain algorithm for solving full vector Maxwell's equations," *IEEE Trans. Microwave Theory Tech.*, vol. 48, pp.1743–1748, Oct. 2000.

[5] J. Chen and J. Wang, "Error between unconditionally stable FDTD methods and conventional FDTD method," *Electon. Lett.*, vol. 42, pp. 1132-1133, Sep. 2006.

[6] J. Chen and J. Wang, "PEC condition implementation for the ADI-FDTD method," *Microwave Opt. Tech. Lett.*, vol. 49, pp. 526-530, Mar. 2007.

[7] J. Chen and J. Wang, "A 3D hybrid implicit-explicit FDTD scheme with weakly conditional stability," *Microwave Opt. Technol. Lett.,* vol. 48, pp. 2291-2294, Nov. 2006.

[8] J. Chen and J. Wang, "Comparison between HIE-FDTD method and ADI-FDTD method," *Microwave Opt. Technol. Lett.,* vol. 49, pp. 1001-1005, May 2007.

[9] J. Chen and J. Wang, "A three-dimensional semi-implicit FDTD scheme for calculation of shielding effectiveness of enclosure with thin slots," *IEEE Trans. Electromagn. Compat.,* vol. 49, pp. 354-360, May 2007.

[10] J. Chen and J. Wang, "Numerical simulation using HIE–FDTD method to estimate various antennas with fine scale structures," *IEEE Trans. Antennas Propagat.*, vol. 55, pp. 3603-3612, Dec. 2007.

[11] I. Ahmed and E. Li, "Conventional perfectly matched layer for weakly conditionally stable hybrid implicit and explicit-FDTD method," *Microwave Opt. Technol. Lett.*, vol. 49, pp. 3106-3109, Dec. 2007.

[12] J. Chen and J. Wang, "Implementation of connection boundary for HIE-FDTD method," *Microwave Opt. Technol. Lett.*, vol. 50, pp. 1347-1352, May 2008.

[13] J. Chen and J. Wang, "The body-of-revolution hybrid implicit-explicit finite-difference time-domain method with large time step size," *IEEE Trans. Electromagn. Compat.*, vol. 50, pp. 369-374, May 2008.

[14] F. Xiao, X. Tang, and L. Wang, "Stability and numerical dispersion analysis of a 3D hybrid implicit-explicit FDTD method," *IEEE Trans. Antennas Propag.,* vol. 56, pp. 3346-3350, Oct. 2008.

[15] J. Chen and J. G. Wang, "Weakly conditionally stability FDTD scheme with reduced split error," *Electron. Lett.*, vol. 42, pp.1017-1019, Aug. 2006.

[16] J. Chen and J. G. Wang, "A novel 3-D FDTD method with weakly conditional stability," *Electron. Lett.*, vol. 43, pp. 2-3, Jan. 2007.

[17] J. Chen and J. Wang, "A novel WCS-FDTD method with weakly conditional stability," *IEEE Trans. Electromagn. Compat.*, vol. 49, pp. 419-426, May 2007.

[18] J. Chen and J. Wang, "Using WCS-FDTD method to simulate various small aperture-coupled metallic enclosures," *Microwave Opt. Technol. Lett.*, vol. 49, pp.

1852-1858, Aug. 2007.
[19] J. Chen and J. Wang, "A new method to avoid the reduction of the time step in CP-FDTD method," *IEEE Trans. Antennas Propag.,* vol. 55, pp. 3613-3619, Dec. 2007.
[20] J. Chen and J. Wang, "A novel body-of-revolution finite-difference time-domain method with weakly conditional stability," *IEEE Microwave Wire Comp. Lett.,* vol. 16, pp. 377-379, Jun. 2008.
[21] R. Luebbers, F. P. Hunsberger, K. S. Kunz, R. B. Standler, and M. Schneider, "A frequency-dependent finite-difference time-domain formulation for dispersive materials," *IEEE Trans Electromagn. Compat*, vol. 32, pp. 222-227, Aug. 1990.

**Juan Chen** was born in Chongqing, China, in 1981. She received the B.S. degree in Public Security Protection Engineering from Chinese People Public- Security University, Beijing, China in 2003 and the Ph.D. degree in electromagnetic field and microwave techniques from Xi'an Jiaotong University, Xi'an, China in 2008. She now serves as a lecturer in the School of Electronic and Information Engineering, Xi'an Jiaotong University. Her research interests are the numerical electromagnetic methods, antenna designs, and electromagnetic compatibility.

**Jianguo Wang** was born in Jiangsu Province, China, on December 21, 1965. He received the B.S. degree in physics from Nanjing University, Nanjing, China in 1987 and the M.S. degree in physics from the Northwest Institute of Nuclear Technology (NINT), Xi'an Shaanxi, China in 1990, and the Ph.D. degree in electromagnetic theory and microwave techniques from Xidian University, Xi'an, Shaanxi, in 1997. From 1998 to 2000, he conducted his postdoctoral research at the Department of Electrical and Computer Engineering, University of Illinois at Urbana-Champaign. He now serves as a professor at NINT. He also works part-time as a Professor in the School of Electronic and Information Engineering, Xi'an Jiaotong University, Xi'an, China. His research interests mainly include transient electromagnetics, numerical electromagnetic methods, antenna designs, and plasma physics.